

Vacancy Clusters in α -Iron*

J. R. BEELER, JR.†

General Electric Company, Cincinnati, Ohio

AND

R. A. JOHNSON

Brookhaven National Laboratory, Upton, New York

(Received 21 October 1966)

A mathematical lattice model was used to compute the kinetic and static aspects of vacancy-cluster nucleation, growth, and dissociation in α -iron. Persistent attention is paid to the kinetics of changes among metastable configurations as well as the formation of stable configurations. The tetravacancy was the smallest immobile vacancy cluster and the mono-, di-, and trivacancy essentially share a common migration-energy value (0.65–0.70 eV). There exists a well-defined hierarchy of different types of stable clusters, the most stable structure being compact clusters, followed in order of decreasing stability by double layers, linear chains, tetravacancies, single layers, trivacancies, and divacancies. The gain in binding energy per additional vacancy increased as the cluster size increased from two to six vacancies. Between 6 and 10 vacancies this gain approached an upper limit of about 0.8 eV/vacancy and remained at this value for larger clusters.

1. INTRODUCTION

A THEORETICAL description of vacancy cluster nucleation, growth, and removal, either by thermally activated dissociation or by conversion into dislocation loops, is of interest with regard to the behavior of worked, quenched, or irradiated metallic specimens. This paper treats certain kinetic and static aspects of vacancy cluster nucleation, growth, and removal in pure α -iron. Considerations pertinent to vacancy cluster nucleation properties are treated in a description of the binding energy as a function of cluster size for each of three classes of cluster structure. Cluster growth is considered in a discussion of the attachment energy of a vacancy to different types of cluster surface facets and the most likely migration path of a vacancy which encounters a cluster. Finally, calculations on the activation energy for cluster dissociation and an unsuccessful attempt to simulate the collapse of planar clusters are discussed.

This study was motivated by the authors's need for a detailed characterization of the static and kinetic properties of vacancy aggregates for use as a basis for a computer simulation of defect annealing in quenched and irradiated specimens. In this regard, the principal properties of interest are: (1) the geometry of the most stable bound configurations, (2) the binding energy of any given cluster configuration, (3) the activation energy for a transition from one cluster configuration to another, and (4) the activation energy for the unit step in the movement process of a given type of mobile cluster. The function of a cluster as a nucleation center for the growth of larger clusters is largely determined by its geometrical configuration and size. These charac-

teristics also determine its effectiveness as a radiation-hardening agent in that asymmetrical defects of a certain appropriate size are believed to be the strongest barriers to dislocation movement.¹ The stability of a cluster against thermal dissociation is characterized by the derivative of the binding-energy function with respect to the number of vacancies contained in a cluster. Configurational transitions and cluster movement are, of course, the fundamental activities by which defect annealing proceeds.

Although the calculations were motivated by an interest in vacancy-cluster behavior in neutron-irradiated metals, many of the results are directly applicable to the annealing process in quenched body-centered cubic (bcc) specimens and to certain aspects of substitutional solute atom aggregation. Because computer simulation of an annealing process requires a jump-by-jump description of many simultaneous defect migration histories, there is a persistent concern with metastable configurations and simple methods for estimating interaction energies.

The particular cluster configurations which are most important as nucleation centers or as irradiation hardening agents are not known, largely because they are not visible in the electron microscope. Recently, however, several investigators have succeeded in observing small defect clusters in refractory metals by using field-ion microscopy.² This capability for direct observation of small clusters, at a level of resolution equal to atomic dimensions, makes the field-ion microscopy and computer-experiment techniques highly complementary research tools in that they both describe

* Work supported by the U. S. Atomic Energy Commission, and performed in part under Contract No. At (40-1)-2847, Fuels and Materials Development Branch.

† Present address: Nuclear Engineering Department, North Carolina State University, Raleigh, North Carolina.

¹ R. L. Fleischer, in *Strengthening of Metals*, edited by D. Peckner (Reinhold Publishing Corporation, New York, 1964); *J. Appl. Phys.* **33**, 3504 (1962); *Acta Met.* **11**, 203 (1963); **10**, 835 (1962); **8**, 598 (1960).

² M. J. Attardo and J. M. Galligan, *Phys. Rev. Letters* **14**, 641 (1965); *Phys. Status Solidi* (to be published); M. A. Fortes and B. Ralph, *Phil. Mag.* **14**, 189 (1966).

TABLE I. Vacancy-pair binding energy as a function of separation distance d_k . Assume one vacancy to be at (0,0,0) and the other at (x,y,z).

k	(x,y,z)	Binding energy (eV)
1	(1,1,1)	0.131
2	(2,0,0)	0.195
3	(2,2,0)	-0.027
4	(3,1,1)	0.051
5	(2,2,2)	-0.009
6	(4,0,0)	-0.028
7	(3,3,1)	-0.009
8	(4,2,0)	0.011
9	(4,2,2)	0.014
10	(5,1,1)	0.004
10	(3,3,3)	-0.002
11	(4,4,0)	0.001
12	(5,3,1)	0.005
13	(6,0,0)	-0.002
13	(4,2,2)	0.000
17	(4,4,4)	0.001
22	(8,0,0)	0.002

defect structure in the same direct geometrical terms and at the same dimensional scale. Consequently, computer experiments can be extremely useful in suggesting and/or serving in the design of field-ion microscope experiments. Conversely, field-ion microscope observations furnish a direct check on computer experiment results and provide particularly pertinent clues for assaying the validity of the individual features of the particular physical model on which the computer experiment is based.

2. COMPUTATIONAL MODEL

The computations were performed using Johnson's lattice model. This method has been described elsewhere in full detail.³⁻⁵ In short, a roughly spherical inner volume containing ~ 540 atoms, each of which could be moved arbitrarily, was used to simulate the detailed atomic configuration associated with a defect. This inner volume was surrounded by an elastic continuum mantle which served the purpose of representing cohesive volume forces. Both the atoms in the inner volume and the mantle were moved in accordance with forces given by an assumed interatomic potential. As mentioned above, the atoms in the inner volume could be moved arbitrarily, but those embedded in the elastic continuum mantle were constrained to move radially in accordance with the displacement equation of linear, isotropic elasticity theory. The interatomic potential used was derived for α -iron by Johnson and used previously by him in a study of point defects.⁴ All results in the present work are based on 20-25 iteration runs each of which explicitly exhibited convergence in the sense of showing a stable oscillation of the configurational energy about a mean value. An IBM 7094 computer was used for these calculations.

³ R. A. Johnson and E. Brown, Phys. Rev. **127**, 446 (1962).

⁴ R. A. Johnson, Phys. Rev. **134**, A1329 (1964).

⁵ R. A. Johnson, Phys. Rev. **145**, 423 (1966).

3. CLUSTER NOTATION

A vacancy cluster in α -iron will be defined as a collection of vacancies in which each member is within a second-neighbor distance of at least one other member. This definition covers the important stable configurations but does not cover certain metastable configurations associated with the reorientation and/or migration of stable configurations. A definition which embraces both stable and metastable configurations can be obtained by replacing the second-neighbor-distance condition in the definition for stable clusters with a fourth-neighbor-distance condition.

It is convenient to classify n -vacancy configurations in terms of the vacancy-pair separation vectors involved. In this regard, the number of vacancy pairs in an n -vacancy configuration is

$$P(n) = \frac{n!}{2!(n-2)!}. \quad (1)$$

We will use d_k to represent the distance between two vacancies which are k th neighbors. Now assume a coordinate system in which the origin is a lattice site and the unit of length is one-half of the lattice constant. Given the coordinates of the vacant sites in an n -vacancy configuration, one can write down a designation M consisting of $P(n)$ digits arranged in order of ascending magnitudes. These digits are the subscripts of the $P(n)$ pair separation vectors $\{\mathbf{d}_k\}$ for the configuration concerned. M will be called the configuration number.

As an example of using the above notation, consider a pair of vacancies separated a distance⁶ d_2 . In this instance, $M = (2)$ and the pair is designated as $v_2(2)$. A trivacancy composed of vacancies at (0,0,0), (0,2,0), and ($\bar{1}$,0,1) is characterized by $M = (112)$ since the pair-separation distances involved are d_1 , d_1 , and d_2 . A trivacancy composed of vacancies at (0,0,0), (0,2,0), and ($\bar{2}$,2,2) involves pair-separation distances d_2 , d_3 , and d_5 . It is designated as $v_3(235)$. Finally, a tetra-vacancy with members at (0,0,0), (0,2,0), (1,1,1), and ($\bar{1}$,1,1) is characterized by the six pair-separation distances d_1 , d_1 , d_1 , d_1 , d_2 , and d_2 . This vacancy tetrahedron is denoted by $v_4(111122)$. One can closely estimate the binding energy of any n -vacancy configuration, given M and the vacancy-pair interaction energies, by algebraic addition of the interaction energies for the vacancy pairs concerned.

4. INTERACTIONS BETWEEN TWO VACANCIES

Johnson⁴ showed that the most stable divacancy configuration in α -iron should be $v_2(2)$. The binding energy of this configuration is 0.195 eV and its migration

⁶ The separation vector is required only when it is necessary to distinguish between configurations such as $\mathbf{d}_{10}(\alpha) = [333]$ and $\mathbf{d}_{10}(\beta) = [511]$, for example.

energy is 0.66 eV. In the present section, the range of interaction between two vacancies is defined as a function of temperature and the activation energies for transitions between various v_2 configurations with separation distances within this interaction range are discussed.

A. Interaction Range

Vacancy-pair binding energies (B) are listed in Table I as a function of the separation distance d_k . Here, as before, d_k is the k th-neighbor separation distance. Denoting the configuration energy of an isolated v_n by $E_c(v_n)$, the binding energy of a v_2 configuration is given by $B = 2E_c(v_1) - E_c(v_2)$. An attractive interaction is indicated by $B > 0$, a repulsive interaction by $B < 0$. Fairly strong repulsive interactions exist for third- and sixth-neighbor separation distances. The three strongest attractive interactions are for second-, first-, and fourth-neighbor separation distances. Except for the d_{12} interaction, all binding-energy magnitudes for separation distances $d > d_{10}$ are small compared with 0.01 eV. It should therefore be a good approximation to neglect the interaction between two vacancies at separations exceeding d_{10} , provided that the temperature lies in the range $T \geq 120^\circ\text{K}$ ($kT \geq 0.01$ eV). In this regard, $d_{10} = 2.6a$, where a is the lattice constant. Depending upon the nature of the physical process concerned, a smaller range of interaction can be assumed, of course, at higher temperatures. In this respect, lower bounds on the vacancy-pair interaction energy magnitudes associated with several vacancy interaction ranges are given in Table II, along with the number of atom sites positioned within each interaction range. The temperature range over which kT exceeds the lower bound on the interaction energy is also specified. Since vacancies appear to migrate in α -iron only at temperatures above 250°C (523°K)⁷ it is certainly permissible, from the standpoint of vacancy interaction influences on vacancy diffusion and association into clusters, to consider that all vacancy interactions vanish for separation distances $d > d_6$. It can then be assumed that as long as a vacancy is separated from any other vacancy by a distance $d > d_6$, its migration mode is a symmetric random walk, whereas the motion of a vacancy separated a distance $d \leq d_6$ from another vacancy is always correlated. It can be seen from Table II that, within the temperature range ($\sim 250^\circ\text{C}$) where vacancy migration begins in α -iron, there are 64 atom sites surrounding each vacancy at which the occurrence of another vacancy would introduce a correlated motion mode for both vacancies. Even at temperatures sufficiently high that only d_1 , d_2 , and d_4 interactions are important, there are still 38 sites in the correlated motion volume about a vacancy. It is significant that the vacancy-vacancy correlated motion volume (64Ω) is comparable to the vacancy-interstitial

⁷ B. L. Eyre and A. F. Bartlett, *Phil. Mag.* **12**, 261 (1965).

TABLE II. Vacancy-vacancy interaction range in α -iron.

Separation-distance range	Number of atom sites	Interaction-energy range
$d \leq d_9$	136	≥ 0.01 eV ($T \geq 120^\circ\text{K}$)
$d \leq d_6$	64	≥ 0.025 eV ($T \geq 290^\circ\text{K}$)
d_1, d_2, d_4	38	≥ 0.05 eV ($T \geq 570^\circ\text{K}$)

recombination volume (40 – 100Ω)^{8,9} in α -iron. The magnitudes and directional dependence of the activation energies for such correlated motion were determined and are presented in Sec. 4 B.

B. Vacancy-Pair Formation and Dissociation

The activation energies for changes among the first nine separation-distance configurations are given in Fig. 1. The large encircled numbers centered in each box are configuration numbers (M). Each arrowhead points to the activation energy required for a transition *to* the configuration number in the box also indicated by the arrowhead, *from* the configuration number in the box indicated by the arrowhead at the opposite end of the connecting line concerned. In the case of a $v_2(2) \rightarrow v_2(4)$ transition, for example, the activation energy is 0.65 eV, while that for the apposite transition, $v_2(4) \rightarrow v_2(2)$, is 0.50 eV. The $v_2(2) \rightarrow v_2(4)$ transition is the initial step in the $v_2(2)$ migration mechanism while the $v_2(4) \rightarrow v_2(2)$ transition completes the process.⁴

Any vacancy-pair configuration can be converted to $v_2(2)$, the most stable v_2 configuration, by a sequence of configurational transitions which involves no repulsive interactions and which exhibits a monotonic increasing sequence of binding energies. This circumstance depends only on the content of Table I and the geometry of the bcc lattice. For example, $v_2(9)$ can change to $v_2(4)$, and $v_2(4)$ to $v_2(2)$, according to Fig. 1. The only import of the repulsive interaction for $v_2(3)$ and $v_2(6)$ is that these

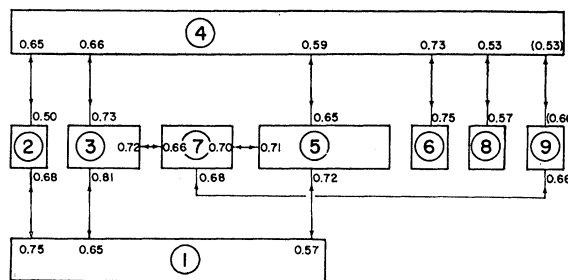


FIG. 1. Activation energies for vacancy-pair configuration change. The large encircled numbers are configuration numbers (M); the small numbers are activation energies in eV. The activation energy for the change from $M=2$ to $M=4$ is 0.65 eV and that for the apposite transition is 0.50 eV, for example.

⁸ C. Erginsoy, G. H. Vineyard, and A. Englert [*Phys. Rev.* **133**, A595 (1964)] treat the vacancy-interstitial recombination volume at 0°K .

⁹ J. R. Beeler, Jr. [*Phys. Rev.* **150**, 470 (1966)] attempts to treat the effective growth of the vacancy-interstitial recombination volume as a function of temperature.

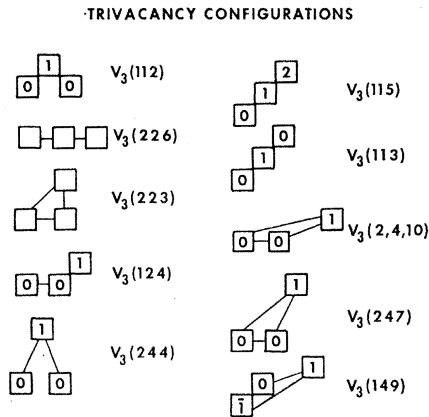


FIG. 2. The ten most stable trivacancy configurations. These configurations would be important in a computer simulation of vacancy annealing in α -iron.

particular configurations will be avoided in the aggregation process. Their existence should in no way impede the formation of stable vacancy pairs.

When the populations of the various two-vacancy configurations are thermal equilibrium state populations, the dissociation energy of a vacancy pair is the sum of its binding energy and the migration energy for an isolated monovacancy. For this case, the dissociation energies for v_2 configurations can be estimated from Table I by adding Johnson's computed value (0.68 eV)⁴ for the vacancy migration energy to the stated binding energy. In the particular case of $v_2(2)$, the dissociation energy estimate is 0.88 eV. This dissociation energy is pertinent to a rate-equation treatment of defect annealing, such as that of de Jong and Koehler.¹⁰ Additional information is required, however, to carry through a computer simulation of vacancy annealing starting from an arbitrary initial defect population, such as that in a displacement spike. In this case, one is concerned with a rather large defect concentration and, consequently, many instances of correlated vacancy motion. Recalling that the vacancy-vacancy correlated motion volume is 64Ω , one sees that when the vacancy concentration is ~ 1.5 at. %, all vacancy motion is correlated. For the particular case of vacancy-pair configuration changes, this correlated motion is completely specified by the activation-energy relationships in Fig. 1.

5. INTERACTIONS AMONG THREE VACANCIES

The most stable trivacancy configuration given by the calculations for α -iron was $v_3(112)$. This isosceles-triangle configuration is particularly interesting because it can migrate without dissociating, a feat which is impossible for the most stable v_3 configuration (equilateral triangle) in face-centered cubic (fcc) structures. In addition, the computed migration energy of $v_3(112)$ is very close to the monovacancy and divacancy migration energies. This mobility of $v_3(112)$ allows it to act as

a building unit in vacancy-cluster formation. Although the discussion is centered on a description of the characteristics of $v_3(112)$, metastable configurations involved in the formation and dissociation of $v_3(112)$ are also treated.

A. Bound Configurations

When internal structure is ignored, a configuration of n vacancies v_n is considered to be a bound configuration provided that its configuration energy $E_c(v_n)$ is less than $nE_c(v_1)$; in this instance, the structure-independent binding energy $B = nE_c(v_1) - E_c(v_n)$ is referred to a state of n independent vacancies. However, a configuration which contains more than two vacancies may be bound in the sense that $E_c(v_n) < nE_c(v_1)$ and yet be composed of two or more well-defined subconfigurations whose net interaction is mutual repulsion. From the standpoint of vacancy aggregate formation and dissociation, it is, of course, necessary to identify and characterize such configurations. For this reason, we state both the structure-independent binding energy B for a vacancy triplet and a structure-dependent binding energy B_s , which is the difference between B and the binding energy of the most tightly bound v_2 configuration contained in the triplet. B_s is thus the binding energy referred to a state of two independent defects, a v_2 and a v_1 . It follows that the activation energy for the dissociation of the triplet into v_2 and v_1 is the sum of B_s and the vacancy migration energy of an isolated vacancy. Since the migration energy of an isolated vacancy is a constant, B_s is a direct measure of v_3 stability against dissociation into v_2 and v_1 .

The configuration and binding energy of each v_3 studied is specified in Table III. For sake of clarity, several of the configurations are illustrated by drawings in Fig. 2. In most of the drawings, a number appears

TABLE III. Trivacancy configurations and their binding energies. Binding energies are given in eV.

Type	B	B_s
(112)	0.489	0.294(2) ^a
(226)	0.386	0.191(2)
(223)	0.364	0.169(2)
(124)	0.340	0.145(2)
(244)	0.290	0.095(2)
(115)	0.267	0.136(1)
(113)	0.251	0.120(1)
(2,4,10)	0.250	0.055(2)
(247)	0.237	0.042(2)
(149)	0.196	0.065(1)
(2,8,11)	0.207	0.012(2)
(2,8,14)	0.206	0.011(2)
(259)	0.200	0.005(2)
(145)	0.163	0.032(1)
(134)	0.147	0.016(1)

^a (2) denotes B_s with respect to $v_2(2)$ and (1) denotes B_s with respect to $v_2(1)$.

¹⁰ M. de Jong and J. S. Koehler, Phys. Rev. **129**, 40 (1963).

inside each vacancy symbol. This number is the z coordinate of the vacancy concerned in half-lattice-constant units. If the configuration is a planar configuration, each vacancy has the same z coordinate and no z designation is necessary and none is designated. These drawings perhaps give a better immediate feel for the shapes involved than does the formal notation introduced in Sec. 3. Because $v_2(2)$ has a larger binding energy than does $v_2(1)$, B_s was computed with respect to $v_2(2)$ unless the triplet contained no $v_2(2)$. In the latter case, it was computed with respect to $v_2(1)$. No triplets were considered which contained neither a $v_2(2)$ nor a $v_2(1)$.

B. v_3 Configuration Change

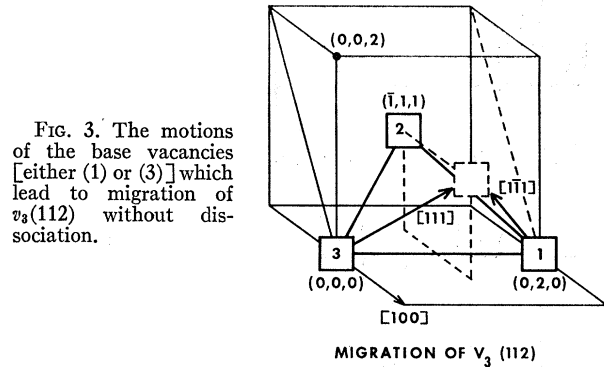
Activation energies are listed in Table IV for the seven configurational changes which $v_3(112)$ can undergo as a consequence of one vacancy jump. Results are given for both the forward transformation (\rightarrow) of $v_3(112)$ into $v_3(ijk)$ and the reverse transformation (\leftarrow) of $v_3(ijk)$ into $v_3(112)$. In addition, the binding energies B_s for the configurations into which $v_3(112)$ can be transformed via a one-jump process appear in the rightmost column of Table IV. Subscripts a and b in the leftmost column indicate the type of vacancy in the $v_3(112)$ triangle which makes the jump in the forward transformation to $v_3(ijk)$: a indicates the apex vacancy and b indicates one of the two equivalent base vacancies. With regard to the dissociation of a $v_3(112)$ into the products $v_2(2)$ and v_1 , the initial process appears to be $v_3(112) \rightarrow v_3(124)$. The initial process for dissociation into products $v_2(1)$ and v_1 appears to be $v_3(112) \rightarrow v_3(145)$. Both of these initial steps in the dissociation process and the migration of $v_3(112)$ without configurational change have the same activation energy. Activation-energy calculations for the dissociation schemes of the six metastable v_3 configurations in Table IV were not performed.

C. Migration of $v_3(112)$

Of the seven most tightly bound trivacancies only $v_3(112)$ can migrate without changing its shape. This being the case, the v_3 migration computations were

TABLE IV. Activation energy for $v_3(112)$ configurational change. One-jump process.

Configuration change	Activation energy (eV)		B_s (eV)
	\rightarrow	\leftarrow	
$v_3(112)_b \leftrightarrow v_3(112)$	0.66	0.66	0.294
$v_3(112)_a \leftrightarrow v_3(223)$	0.80	0.68	0.169
$v_3(112)_b \leftrightarrow v_3(124)$	0.66	0.51	0.145
$v_3(112)_b \leftrightarrow v_3(113)$	0.96	0.72	0.120
$v_3(112)_b \leftrightarrow v_3(145)$	0.66	0.34	0.032
$v_3(112)_a \leftrightarrow v_3(235)$	0.88	0.54	-0.034
$v_3(112)_b \leftrightarrow v_3(134)$	0.80	0.60	0.016



limited to the $v_3(112)$ configuration. For purposes of discussion, we will consider the particular instance of a $v_3(112)$ lying in a (101) plane, as in Fig. 3. This cluster can migrate along either $[1\bar{1}1]$ or $[\bar{1}1\bar{1}]$ as a consequence of base vacancy (1) moving an interatomic distance (unit jump) in these directions. Similarly, the cluster can move along either $[111]$ or $[\bar{1}\bar{1}\bar{1}]$ as a consequence of base vacancy (3) making a unit jump along $[111]$ or $[\bar{1}\bar{1}\bar{1}]$. Movement of the apex vacancy (2) and any movement of a base vacancy in the plane of $v_3(112)$ leads to a change in shape. The centroid of $v_3(112)$ moves a distance $\sqrt{3}(a/6)$ at each jump. The migration energy for $v_3(112)$ is 0.66 eV, while the migration energy for v_2 is also 0.66 eV and that for v_1 is 0.68 eV. It thus appears that v_1 , v_2 , and v_3 migrate with about the same migration energy in α -iron.

There are 12 distinct $v_3(112)$ orientations, consisting of the eight $v_3(112)$ facets of the bcc octahedron and the four $v_3(112)$ appearing in the diagonal planes of this polyhedron. It is possible for a $v_3(112)$ to move along $\langle 100 \rangle$, $\langle 110 \rangle$, and $\langle 111 \rangle$ in a correlated series of vacancy jumps in which a given orientation is repeated in either a three-jump or six-jump cycle. In particular, the orientation in Fig. 3 repeats every third jump along $[111]$ and six-jump cycles exist which cause it to repeat along $[010]$ and $[101]$. This circumstance gives $v_3(112)$ a great deal of flexibility in both approach and attachment to a larger cluster. It could serve, clearly, as a building unit in the formation of large clusters.

6. INTERACTION AMONG FOUR VACANCIES

The most stable tetravacancy configuration was the $v_4(111122)$ tetrahedron, which had a binding energy of 1.023 eV. This cluster cannot migrate without dissociating into (v_3+v_1) , the activation energy for this particular dissociation process being about 1.2 eV. Because of its immobility, $v_4(111122)$ is not so interesting a defect as the very versatile $v_3(112)$ which can serve as a vehicle for vacancy transport, a tightly bound mobile building unit for cluster formation and a sink for monovacancies and divacancies. The leading role of the most stable v_4 configuration is that of being a firm nucleation center for vacancy-cluster growth.

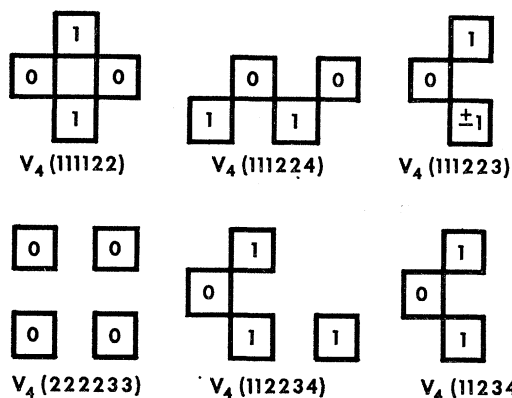


FIG. 4. v_4 configurations for which binding-energy calculations were made in this study.

Configurational-energy calculations were made for six v_4 configurations which included the $v_4(111122)$ tetrahedron, the $v_4(111224)$ parallelogram, and the $v_4(222233)$ square. The parallelogram and square configurations are the most stable planar v_4 clusters in $\{110\}$ and $\{100\}$ planes, respectively. Drawings of these six clusters appear in Fig. 4. A description of the 12 most tightly bound v_4 configurations is given in Table V. The additivity approximation was used to obtain B and B_s in three instances, as is indicated. In the top four entries, B_s exceeds 0.294 eV, the value of $B_s[v_2(2) - v_1]$ for $v_3(112)$; in the middle four entries it exceeds 0.195 eV, the value of $B_s[v_1 - v_1]$ for $v_2(2)$. Hence, the cluster stability ranges from the stability of $v_3(112)$ to that for $v_4(111122)$ in the first group of v_4 configurations. In the second group of v_4 configurations, it ranges from the stability of $v_2(2)$ to the stability of $v_3(112)$. Configurations in the last group are less stable than $v_2(2)$. Activation energies for the first vacancy jump and $B_s(v_3 - v_1)$ values for the resulting v_4 are given in Table VI for possible schemes for the dissociation of $v_4(111122)$ into $v_3(112)$ and v_1 .

7. LARGER CLUSTERS

Following a characterization of the mobile stable clusters and of $v_4(111122)$, the smallest immobile stable

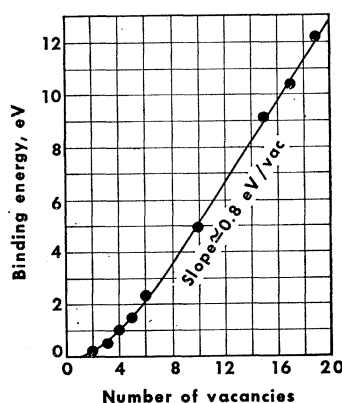


FIG. 5. Binding energy of the most stable vacancy cluster of n vacancies as a function of n . (See caption of Fig. 6.)

TABLE V. Tetravacancy configurations in α -iron and their binding energies (in eV).

Type	B	B_s	
(111122)	1.023	0.534	
(111224)	0.844	0.355	
(111223)	0.788	0.299	
(112244) ^a	0.786	0.297	
(222233)	0.749	0.285 ^b	(0.294)
(111123) ^a	0.714	0.225	
(112234)	0.708	0.219	
(112246) ^a	0.707	0.218	
(111245)	0.662	0.173	(0.195)
(111234)	0.644	0.155	
(112448)	0.602	0.113	
(111235)	0.584	0.095	

^a B and B_s obtained using the additivity approximation.
^b $B_s(v_3 - v_1)$ for $v_4(222233)$ is referred to $v_3(223)$, the $B_s(v_3 - v_1)$ entries for all other v_4 listed are referred to $v_3(112)$.

cluster, one's interest naturally turns to the ways in which large clusters could build up from a v_4 nucleus during vacancy migration. In this regard, the computations indicate that linear, planar, and volumed (compact) cluster forms could occur which are more stable

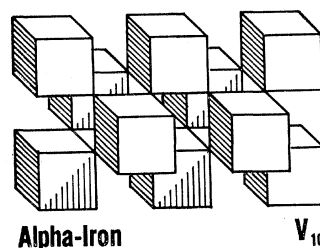


FIG. 6. Structure of the most stable v_{10} cluster; a linear chain of crossed $v_2(2)$ pairs. This type of structure is the most stable structure for $n \leq 10$. The compact structure is the most stable structure for larger clusters.

than $v_4(111122)$. The specific planar forms which possess greater stability than $v_4(111122)$ are double-layer platelets. In addition to double-layer platelets, single-layer platelets parallel to $\{110\}$ planes could exist whose stability lies between that of $v_3(112)$ and $v_4(111122)$ and single-layer platelets parallel to $\{100\}$ planes could exist whose stability slightly exceeds that of $v_3(112)$. In short, the hierarchy of cluster stability, in descending order of degree appears to be: (1) compact clusters, (2) double-layer platelets, (3) linear chains of either $v_2(2)$ or $v_3(112)$ units, (4) $v_4(111122)$, (5) single-layer platelets parallel to $\{110\}$ planes, (6) single-layer platelets parallel to $\{100\}$ planes, (7) $v_3(112)$, and (8) $v_2(2)$.

TABLE VI. Dissociation of $v_4(111122)$ into $v_3(112)$ and v_1 .

Initial process	First stage		Product B_s eV
	Activation energy (eV)		
	(\rightarrow)	(\leftarrow)	
$v_4(111122) \rightarrow v_4(111223)$	0.82	0.55	0.299
$v_4(111122) \rightarrow v_4(112345)$	0.86	0.31	0.015
$v_4(111122) \rightarrow v_4(112234)$	0.82	0.47	0.219

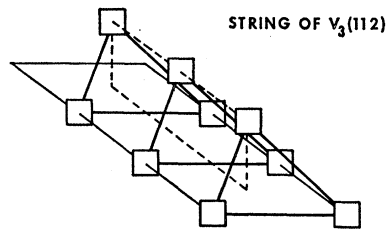
TABLE VII. Coefficients α and β in the binding energy expression $B = \alpha n - \beta$ for vacancy clusters in α -iron.

Cluster type	α , eV	β , eV
Compact	0.79	2.85
{110} double layer	0.77	3.05
{100} double layer	0.62	2.30
Linear chains	0.6	...
v_4	0.53	...
{110} monolayer	0.43	1.30
{100} monolayer	0.32	1.10
v_3	0.29	...

A. Binding Energy

Binding-energy computations were made for compact clusters containing as many as 19 vacancies. The binding energy of the most stable compact cluster of n vacancies is plotted in Fig. 5. For $n \geq 10$, the binding energy is a linear function of n with a slope of 0.79 eV/vacancy, and is given by the relation $B = (0.79n - 2.85)$, in eV, for $n \geq 10$.

Double-layer platelets parallel to {110} planes had binding energies which were nearly as large as the binding energies of compact clusters containing the

FIG. 7. Linear chain of $v_3(112)$ configurations.

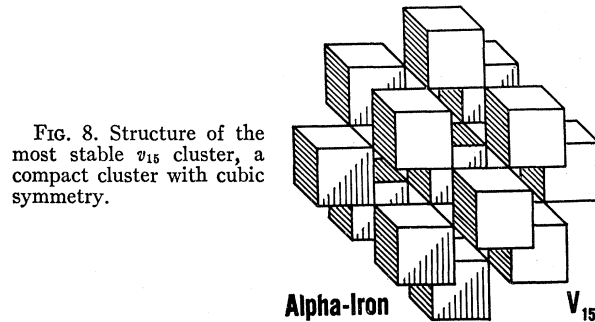
same number of vacancies. The binding energies of {100} double layers or of linear chains (Figs. 6 and 7) were each about 20% lower than that of a compact cluster containing the same number of vacancies. In all instances, it was possible to express the binding energy in the form

$$B = \alpha n - \beta, \quad (n \geq 10), \quad (2)$$

where α and β are given by Table VII in eV. The coefficient of n , i.e., $\alpha = dB/dn$, is B_s and, therefore, is a direct measure of cluster stability. The ranking of degrees of stability given in the introduction to this section is seen to follow directly from Table VII.

TABLE VIII. Vacancy-cluster dissociation energies in α -iron.

Process	Dissociation energy (eV)
$v_2(2) \rightarrow v_1 + v_1$	0.88
$v_3(112) \rightarrow v_2(2) + v_1$	0.97
$v_4(111122) \rightarrow v_3(112) + v_1$	1.21
$v_6(\text{compact}) \rightarrow v_5(\text{compact}) + v_1$	1.46
$v_n(\text{compact}) \rightarrow v_{n-1}(\text{compact}) + v_1$	1.47 ^a

^a For $n > 6$.FIG. 8. Structure of the most stable v_{15} cluster, a compact cluster with cubic symmetry.

The most simple linear chain is a sequence of crossed $v_2(2)$ pairs centered on a {100} axis. A v_{10} configuration with this structure appears in Fig. 6. The limiting value of the binding-energy gain per added vacancy is about 0.6 eV for this type of chain. Another possible linear chain is a sequence of $v_3(112)$ configurations such as that illustrated in Fig. 7. Here too, the binding energy gain per vacancy added is about 0.6 eV. These linear chains are quite stable and should persist at temperatures sufficiently high to dissociate v_4 and v_3 clusters, the stabilities of these two smaller defects being at most 0.53 and 0.29 eV, respectively.

B. Bound Configurations

The most stable configurations for clusters of ≤ 10 vacancies can be obtained from Fig. 6. For example, that for v_9 is found by removing the upper right vacancy in Fig. 6, that for v_8 by removing the two right-most vacancies in the figure and so forth for v_7 , v_6 , and v_5 . It would seem that linear chains of this type could form quite easily, since the $v_2(2)$ migration energy is 0.66 eV and its dissociation energy is considerably larger (0.88 eV). Although the linear-chain systems discussed thus far have been straight, one observes that they can adopt a structure which contains 90° bends with no loss

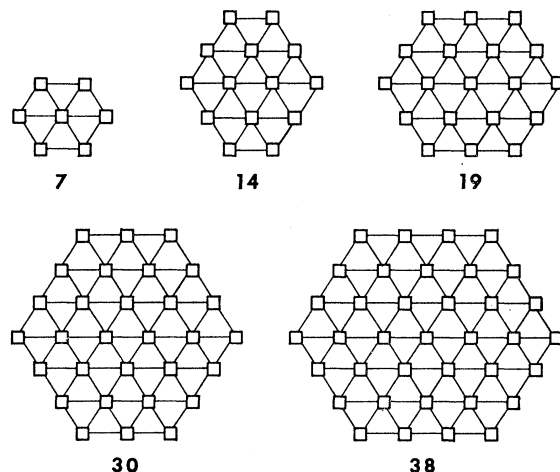


FIG. 9. One set of {110} single-layer platelets used in the attempt to obtain a vacancy loop via platelet collapse. Triangular and parallelogram platelet shapes were also considered.

in binding energy; indeed, such bends will, in fact, slightly increase the binding energy toward that characteristic of double layers and compact clusters.

Linear chains of $v_3(112)$ triads (Fig. 7) are not only energetically stable but could in fact be formed solely as the result of $v_3(112)$ migration. This follows from the circumstances that $v_3(112)$ can migrate without first dissociating and possesses complete orientational flexibility. These chains could also serve as nuclei for large compact clusters such as the v_{15} in Fig. 8. This cluster has cubic symmetry and can be built up by aggregation of v_1 and $v_3(112)$ units. It cannot be built up solely by the aggregation of $v_2(2)$ pairs.

Vacancy cluster dissociation energies are summarized in Table VIII for the most tightly bound configurations and for the dissociation scheme $v_n \rightarrow v_{n-1} + v_1$. Other dissociation schemes were always found to give higher dissociation energies.

C. Platelet Collapse

An attempt was made to simulate vacancy platelet collapse into a vacancy loop, but the venture was not successful. In the case of a single-layer platelet, a slight tendency for a drawing together of the platelet faces at corners and edges was exhibited for clusters of $10 < n < 37$ vacancies, but no hint of an impending total collapse was detected. In fact, the roof and floor of the platelet always tended to draw away from each other at the center of the platelet. Some of the platelets investigated are shown in Fig. 9. Platelets in the shape of triangles and parallelograms were also considered.

8. SUMMARY AND CONCLUSIONS

Vacancy-cluster configurations, binding energies, migration energies, and dissociation energies in α -iron were computed using Johnson's lattice model. The primary results of these calculations are:

- (1) For any vacancy cluster size, a stable configuration could be found with a greater binding energy than any smaller cluster.
- (2) There exists a well-defined hierarchy of different types of stable clusters, the most stable structure being compact clusters followed in order of decreasing stability by double layers, linear chains, tetravacancies, single layers, trivacancies, and divacancies.
- (3) The gain in binding energy per additional vacancy increased as the cluster size increased from two to six vacancies. Between 6 to 10 vacancies, this gain approached an upper limit of 0.8 eV/vacancy and remained at this value for larger clusters.
- (4) Essentially the same migration energy was found for v_1 , v_2 , and v_3 . This is of importance with respect to the interpretation of vacancy-annealing data in that although each of these defects will have a different diffusion coefficient they should exhibit a common diffusion activation energy.
- (5) In order to migrate, the tetravacancy must first dissociate. In effect, it is the smallest immobile nucleus for vacancy-cluster formation, since the activation energy for v_4 dissociation is 1.2 eV.

The binding energy of any vacancy configuration can be closely approximated (within 10%) by the summation of all the vacancy-pair interaction energies in the configuration. This approximation is sufficiently reliable that one can compare the stability of two arbitrary configurations using the data given in Table I. An attempt was made to consider all of the most important stable configurations, but clearly not all conceivable types of vacancy configurations could be calculated. Particular cases of interest not covered in this study can be treated using the pairwise interaction approximation described above.

ACKNOWLEDGMENTS

The authors are indebted to Nancy R. Baumgardt for modifying the original computer program so as to automate migration-energy calculations. The initial-state atomic relaxations about each cluster treated were computed by Mrs. J. M. Neale, who also processed the computer output data.